



# Pulse-resolved beam position measurements of high energy X-ray pulses at MHz rate with a diamond sensor

TUBA ÇONKA YILDIZ,<sup>1,\*</sup> WOLFGANG FREUND,<sup>1</sup> JIA LIU,<sup>1,3</sup> MICHAL POMORSKI,<sup>2</sup> AND JAN GRÜNERT<sup>1</sup>

<sup>1</sup>European XFEL, Holzkoppel 4, Schenefeld, 22869, Germany

<sup>2</sup>Université Paris-Saclay, CEA, LIST, F-9112, Palaiseau, France

<sup>3</sup>jia.liu@xfel.eu

\*tuba.conka@xfel.eu

Received 12 May 2023; revised 28 June 2023; accepted 2 July 2023; published 21 July 2023

**The European X-ray Free Electron Laser facility produces extremely intense and short X-ray pulses. A diamond sensor proposed for non-invasive diagnostics of hard X-rays enables pulse-resolved beam position measurements within less than 1% uncertainty at 2.25 MHz.** © 2023 Optica Publishing Group under the terms of the [Optica Open Access Publishing Agreement](https://doi.org/10.1364/OPTICA.495437)

<https://doi.org/10.1364/OPTICA.495437>

X-ray free-electron lasers (XFELs) generate extremely intense X-ray pulses with durations in the femtosecond range. These pulses are created via a process called self-amplified spontaneous emission (SASE), which has a stochastic feature causing variations in beam intensity, spectrum, and position. Therefore, it is critical to perform single-shot beam intensity and position measurements [1] in the least-invasive manner, during which almost no photons are lost and beam properties are affected as little as possible. There has been previous work demonstrating a curved grating technique in good agreement with the method of ablative imprints in analyzing FEL beam dimensions and properties [2]. However, these measurements were neither non-invasive nor single-pulse resolving. At the European XFEL (EuXFEL) [3], X-ray gas monitor detectors (XGMs) [4] are used for monitoring the pulse-resolved and absolutely calibrated pulse energy signal. Meanwhile the beam position can also be derived, but only averaged over several tens of seconds. For gas-based systems, the efficiency drops as photon energy increases; besides, it is not always possible to implement such bulky systems. X-ray imaging systems [5] deliver accurate beam shape and position information, but only at 10 Hz. To overcome the above issues, sensors have been developed based on single-crystal diamonds produced by chemical-vapor-deposition (CVD), and they were used as beam monitors at synchrotron facilities [6–8]. Thanks to the excellent diamond material performance under high temperature, high frequency, high voltage, and high radiation [9,10], we were able to apply these sensors to the much brighter and shorter XFEL pulses (synchrotrons deliver on the order of  $10^{12}$  photons per second while FELs produce a similar number of photons in each single pulse), demonstrating unprecedented pulse-resolved FEL beam position measurements.

The sensor shown in Fig. 1 has both surfaces covered by diamond-like carbon (DLC) layers with defined resistivity of  $350 \Omega$  on the front and  $750 \Omega$  on the back side, and on each side, two planar metallized electrode strips allow the collection of the generated currents. The sensor consists of an electronic grade diamond with a high charge collection efficiency with dimensions  $4 \times 4 \text{ mm}^2$  with a thickness of  $40 \mu\text{m}$ .

The X and Y position information is calculated using

$$X = \frac{A(x_1) - A(x_2)}{A(x_1) + A(x_2)} \cdot \frac{L}{2}, Y = \frac{A(y_1) - A(y_2)}{A(y_1) + A(y_2)} \cdot \frac{L}{2},$$

where  $A(x_i)$  and  $A(y_i)$  are the X-ray-induced current on lateral electrode  $x_i$  and  $y_i$ , respectively.  $L$  corresponds to the distance between the lateral metal electrodes. A duo-lateral diamond sensor was mounted on an XY motorized manipulator and attached to the K-monochromator [11] vacuum chamber in the X-ray tunnel for distribution (XTD1) of the SASE2 beamline.

First, diamond sensor functional tests were performed at 12 – 15 keV and 30 keV. The recent results that we present here were obtained at a photon energy of 11 keV. The beam arriving at the diamond contained a train of 30 pulses at an intra-pulse repetition rate of 2.25 MHz, with the trains repeating at 10 Hz and with an average pulse energy of around  $130 \mu\text{J}$ .

Due to the large signals produced from FEL pulses, a 50 dB attenuator was used for each current signal of the sensor, which was biased with 100 V. The digitization of the signals is performed by FastADC modules in  $\mu$ -TCA crate. These commercial ADCs (FastADC by Struck) have 16-bit resolution and a sampling rate of

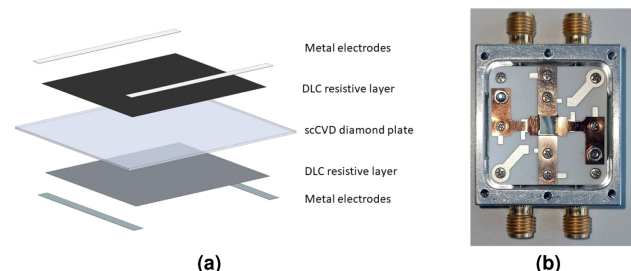


**Fig. 1.** (a) Structure of the diamond sensor and (b) photo of the mounted diamond sensor.

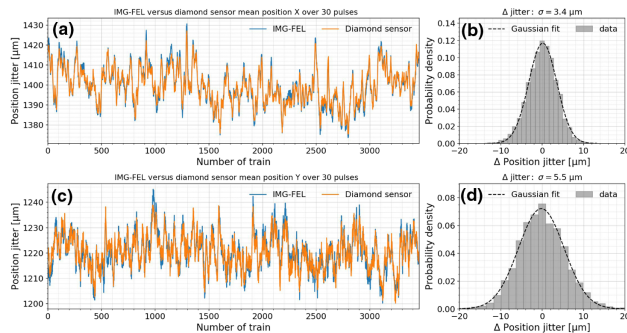


**Fig. 2.** Beam position measured by the diamond sensor and FEL imager in (a) X and (c) Y directions; (b) and (d) are the position differences in X and Y directions, respectively.

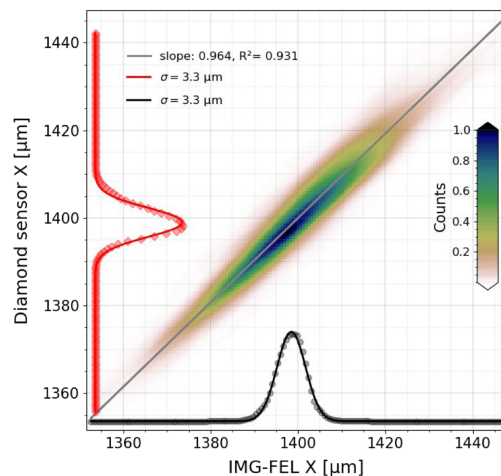


**Fig. 3.** Correlation of X direction beam position measured by the diamond sensor and the FEL imager.

108 MHz. Pulse stretchers in the analog front-end electronics are used to temporally resolve the few ns long pulses with this limited sampling rate. The ADCs are triggered synchronously with each pulse train. The calibration of the sensor was performed by moving the sensor in X and Y directions.

The diamond sensor mean position averaged over all 30 pulses in the train was compared with train-resolved data of the SASE2 FEL imager [5] and is in good agreement as shown in Figs. 2 and 3. Figure 3 demonstrates the direct correlation of the position X measured by both detectors, with the X and Y lineouts extracted from correlation shown as red and black curves. The correlation width of the distribution defines the measurement uncertainty.

As an example, an image of the FEL beam recorded by the FEL imager is shown in Fig. 4 where the red dot represents the 2D tilted Gaussian fitted centroid position of the beam, whereas the green dots are single-shot beam positions measured by the diamond sensor. The ellipse is the contour plot of the fitted 2D profile, and the dashed cross represents the mean position measurement by the diamond sensor measurements, where the average was taken over all pulses in the train.

In conclusion, a diamond sensor was developed for operation with high energy X-ray beams such as those produced at FELs. It

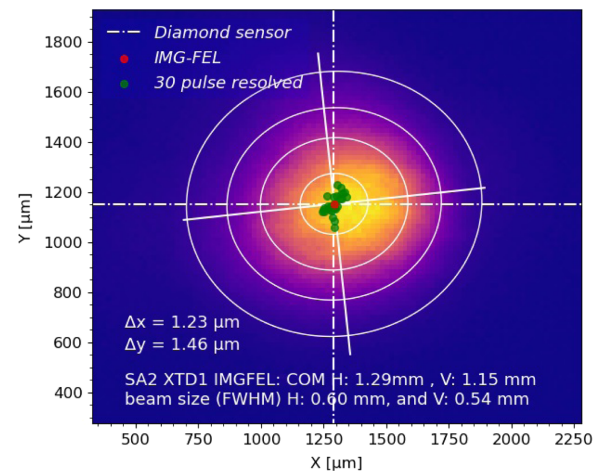


**Fig. 4.** Beam position (X and Y directions) measured with the diamond sensor and the FEL imager.

delivers pulse-resolved beam position information at MHz rate and has a position measurement uncertainty of 3  $\mu\text{m}$  (X-direction) and 5  $\mu\text{m}$  (Y-direction), which corresponds to 0.5% – 1% uncertainty for a beam diameter on the order of 500  $\mu\text{m}$ .

**Funding.** European XFEL GmbH.

**Acknowledgment.** We thank the Electronics and Electrical Engineering (EEE) group of EuXFEL for the modifications they provided at the electronics of the K-monochromator. We also thank the DESY MDI group and the team at the accelerator control room (BKR) for their support.

**Disclosures.** The authors declare no conflicts of interest.

**Data availability.** Data are available upon reasonable request.

## REFERENCES

1. J. Grünert, M. P. Carbonell, F. Dietrich, T. Falk, W. Freund, A. Koch, N. Kujala, J. Laksman, J. Liu, T. Maltezopoulos, and K. Tiedtke, *J. Synchrotron Rad.* **26**, 1422 (2019).
2. G. Mercurio, J. Chalupský, I. T. Nistea, *et al.*, *Opt. Express* **30**, 20980 (2022).
3. W. Decking, S. Abeghyan, P. Abramian, *et al.*, *Nat. Photonics* **14**, 391 (2020).
4. T. Maltezopoulos, F. Dietrich, W. Freund, U. F. Jastrow, A. Koch, J. Laksman, J. Liu, M. Planas, A. A. Sorokin, K. Tiedtke, and J. Grünert, *J. Synchrotron Rad.* **26**, 1045 (2019).
5. A. Koch, J. Risch, W. Freund, T. Maltezopoulos, M. Planas, and J. Grünert, *J. Synchrotron Rad.* **26**, 1489 (2019).
6. M. Pomorski, M. Ciobanu, C. Mer, M. Rebisz-Pomorska, D. Tromson, and P. Bergonzo, *Phys. Status Solidi A* **206**, 2109 (2009).
7. K. Desjardins, M. Bordessoule, and M. Pomorski, *J. Synchrotron Rad.* **25**, 399 (2018).
8. J. Morse, B. Solar, and H. Graafsma, *J. Synchrotron Rad.* **17**, 456 (2010).
9. W. Freund, *Adamas Workshop*, GSI, Germany, 2019.
10. T. Roth, W. Freund, U. Boesenberg, G. Carini, S. Song, G. Lefeuve, A. Goikhman, M. Fischer, M. Schreck, J. Grünert, and A. Madsen, *J. Synchrotron Rad.* **25**, 177 (2018).
11. W. Freund, L. Fröhlich, S. Karabekyan, A. Koch, J. Liu, D. Nölle, J. Wilgen, and J. Grünert, *J. Synchrotron Rad.* **26**, 1037 (2019).